Trinuclear complexes with $Pt_2M(\mu_3\text{-}S)$ groups and the ease of inversion at sulfur

Nasim Hadj-Bagheri and Richard J. Puddephatt*
Department of Chemistry, University of Western Ontario, London, Ont., N6A 5B7 (Canada)

(Received March 1, 1993)

Abstract

The binuclear platinum complex $[Pt_2(\mu\text{-}S)(\mu\text{-dppm})(\eta^1\text{-dppm})_2]$ (**1**), dppm = $Ph_2PCH_2PPh_2$, can act as a tridentate ligand in forming homonuclear and heteronuclear cluster cations. Thus, **1** reacted with square planar complexes of formula $[PtClRL_2]$, $L_2 = (SMe_2)_2$ or 1,5-cyclooctadiene (cod), to form the corresponding trinuclear clusters $[Pt_3R(\mu_3\text{-}S)(\mu\text{-dppm})_3]^+Cl^-$ (R = Me (**2**), Ph (**3**), CH_2Cl (**4**), Cl (**5**)), with $[PdCl_2(PhCN)_2]$ to form $[Pt_2PdCl(\mu_3\text{-}S)(\mu\text{-dppm})_3][Cl]$ (**6**), with $[Rh(\mu\text{-}Cl)(CO)_2]_2$ or $[Ir(\mu\text{-}Cl)(CO)_3]_2$ to form $[Pt_2M(CO)(\mu_3\text{-}S)(\mu\text{-dppm})_3][Cl]$ (M = Rh (**7**), Ir (**8**)), with the d^{10} metal compounds CuCl, $AgNO_3$ and $[AuCl(SMe_2)]$ to give $[Pt_2M(\mu_3\text{-}S)(\mu\text{-dppm})_3]^+$ (M = Cu (**9**), Ag (**10**), Au (**11**)), and with $Hg(NO_3)_2$ to yield $[Pt_2M(\mu_3\text{-SMe})(CO)(\mu\text{-dppm})_3]^{2+}$. Complexes **7** and **8** each reached with excess iodomethane to yield $[Pt_2M(\mu_3\text{-SMe})(CO)(\mu\text{-dppm})_3]I_2$ (M = Rh (**16**), Ir (**17**)) and with $AgBF_4$ to give $[Pt_2(\mu_3\text{-}S)(CO)(\mu_3\text{-AgCl})(\mu\text{-dppm})_3]BF_4$ (M = Rh (**19**), Ir (**20**)). The complexes **2–8** are shown to be fluxional with respect to inversion at sulfur, whereas **9–12** are not; the inversion has a lower activation energy for **7** and **8** than for **2–6** and this is attributed to stabilization of the planar transition state by the carbonyl ligand. The structure of **11** has been confirmed by an X-ray structure determination.

Introduction

The ligands bis(diphenylphosphino)methane (dppm) and sulfide each tend to bridge between late transition metals and so stabilize binuclear and cluster complexes with weak or absent metal–metal bonding [1–6]. Complexes with higher nuclearity can be built up systematically by reactions in which complexes containing $M(\eta^1\text{-dppm})$ or $M_2(\mu_2\text{-}S)$ groups act as ligands to a second metal M′ to give $MM'(\mu\text{-dppm})$ or $M_2M'(\mu_3\text{-}S)$ groups [1–6]. The complex $[Pt_2(\mu\text{-}S)(\mu\text{-dppm})(\eta^1\text{-dppm})_2]$ (**1**) contains both of the above functional groups and is easily prepared by reaction of $[Pt_2(\mu\text{-dppm})_3]$ with carbonyl sulfide [7]. Complex **1** can act either as an 8-electron or 6-electron ligand, using in each case the lone pair on two η^1-dppm ligands and either 2 or 1 lone pair from the μ-S group [7]. This paper reports the more general chemistry of **1** as a 6-electron ligand in forming homonuclear and heteronuclear complexes containing $Pt_3(\mu_3\text{-}S)$ or $Pt_2M(\mu_3\text{-}S)$ cores, M = Rh, Ir, Pd, Cu, Ag or Au. All of these complexes undergo inversion at the μ_3-S center at a rate amenable to study by NMR, and the factors influencing the ease of inversion are discussed. A preliminary account of parts of this work has already been published [8].

*Author to whom correspondence should be addressed.

Results

Synthesis and characterization of triplatinum complexes

The binuclear platinum complex **1** reacted with a series of square planar complexes of the general formula $[PtClRL_2]$, where R = Me, Ph, CH_2Cl or Cl and $L_2 = (SMe_2)_2$ or 1,5-cyclooctadiene (cod), to form the trinuclear clusters $[Pt_3R(\mu_3\text{-}S)(\mu\text{-dppm})_3]^+Cl^-$, as shown in Scheme 1. In these reactions, complex **1** acts as a tridentate ligand in displacing $2L + Cl^-$ from $[PtClRL_2]$. Since the synthetic methods and NMR data are similar for all the triplatinum derivatives, only one example is chosen for a detailed discussion. The NMR data are recorded in Tables 1–3.

Complex **1** reacted easily with *trans*-$[PtClMe(SMe_2)_2]$ in acetone solution to give $[Pt_3Me(\mu_3\text{-}S)(\mu\text{-dppm})_3][Cl]$ (**2**), which was isolated as a yellow solid in almost quantitative yield. The cation is very similar to known cluster cations such as $[Pt_3H(\mu_3\text{-}S)(\mu\text{-dppm})_3]^+$, and so characterization was straightforward, based on the rich ^1H, ^{31}P and ^{195}Pt NMR spectra [9–11].

The ^1H NMR spectrum of **2** contained a PtMe signal at $\delta = -0.46$, which appeared as a triplet of triplets due to PH coupling, with $^3J(PH)$ and $^5J(PH)$ values of 7 and 2 Hz, respectively. Satellites due to coupling to platinum were also observed with $^2J(PtH) = 66$ Hz. Two resonances were observed for the P_2CH_2 protons of

0020-1693/93/$6.00

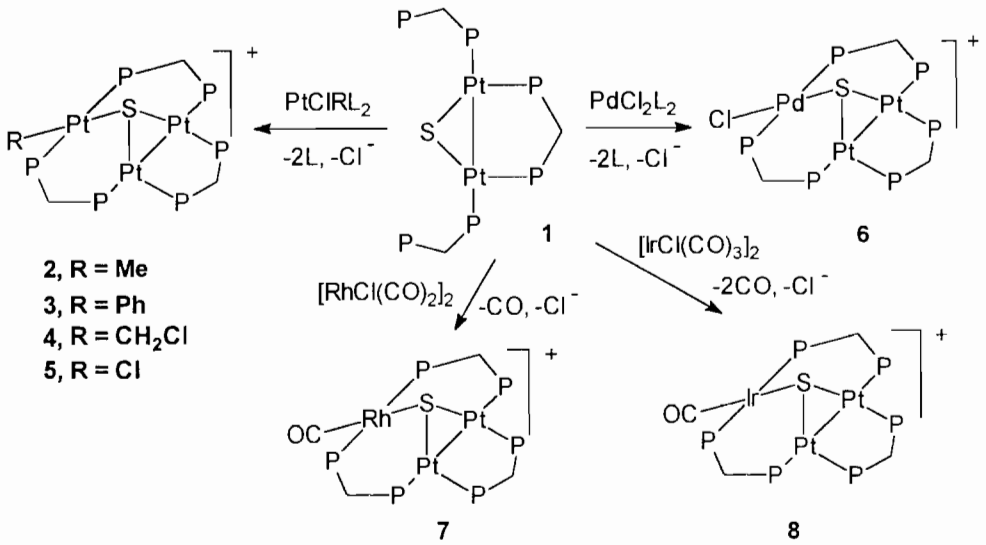

Scheme 1.

TABLE 1. ^{1}H NMR data and ΔG^* values for Pt_3 and Pt_3M clusters

Complex	δ (ppm)	$P_2CH^aH^b$		T_c (°C)	$\Delta\nu$ (Hz)	ΔG^* (kJ mol^{-1})	$P_2CH^cH^d$ δ (ppm)	T_c (°C)	$\Delta\nu$ (Hz)	ΔG^* (kJ mol^{-1})
		^2J(PH) (Hz)	^3J(PtH) (Hz)							
2	4.0	4	41	−20	68	51	5.4	−30	70	49
3	4.1	4	40	−20	112	50	5.3	−20	68	51
5	3.9	4	40	−2	232	52	5.5	−2	206	52
6	4.1	4		−5	85	54	5.5	0	276	52
7	4.2	4		−60	103	42	5.6	−50	320	42
8	4.3	4		−50	91	44	5.6	−45	105	43

TABLE 2. $^{31}P\{^1H\}$ NMR data for Pt_3 and Pt_2M clusters

Complex	δ (P^a) (ppm)	$^4J(P^aP^c)$ (Hz)	$^1J(PtP^a)$ (Hz)	δ (P^b) (ppm)	$^2J(P^bP^a)$ (Hz)	$^3J(P^bP^{b\prime})$ (Hz)	$^1J(PtP^b)$ (Hz)	$^2J(PtP^b)$ (Hz)	δ (P^c) (ppm)	$^1J(PtP^c)$ (Hz)	$^1J(PtP^c)$ (Hz)	$^1J(PtPt)$ (Hz)
[a]	25.2		2992	5.0	27	170	3110	222	−12.7	3887	−80	2620
2	25.4	7	3060	1.7	20	170	3080	210	−12.6	3840	−80	2842
3	20.2	8	3040	−3.2	17	180	3080	170	−11.7	3840	−80	2890
4	23.1	8	3100	1.9	20	170	3080	190	−11.6	3860	−80	2920
5	20.0	7	2780	1.6	21	168	3060	170	−12.5	3872	−80	2761
6	20.8	5		4.8	25	163	3042	150	−9.3	3848	−78	2770
7	26.9	7	130[b]	4.2	32	170	3080	170	−9.3	3920	−68	2485
8	17.6	9		1.3	25	160	3124	180	−10.2	4000	−60	2519
9	−20.4			16.5	70	180	3280	200	−10.8	3840	−120	2842
10	−10.7		400[c]	16.4	70	170	3300	210	−11.9	3560	−80	2355
11	24.5			17.1	70	178	3343	186	−13.2	3634	−89	3146
12	17.2		4460[d]	17.1	70	190	3180	170	−10.8	3720	−80	2665

[a]Data for $[Pt_3H(\mu_3\text{-}S)(\mu\text{-dppm})_3]^+$. [b] ^1J(RhP). [c] ^1J(AgP). [d] ^1J(HgP).

TABLE 3. $^{195}Pt\{^1H\}$ NMR data for Pt_3 and Pt_2M clusters

Complex	δ (Pt^a) (ppm)	$^1J(PtP_a)$ (Hz)	δ (Pt^b) (ppm)	$^1J(Pt^bP^b)$ (Hz)	$^2J(Pt^bP^b)$ (Hz)	$^1J(Pt^bP^c)$ (Hz)	$^2J(Pt^bP^c)$ (Hz)	$^1J(PtPt)$ (Hz)
[a]	−3181	2992	−3172	3110		3887		2620
2	−2991	3060	−3199	3080	210	3840	−80	2840
3	−2833	3050	−3206	3080	180	3850	−80	2890
4	−2645	3100	−3250	3100	170	3860	−80	2910
5	−2533	2780	−3318	3070	160	3870	−80	2760
6			−3123	3050	150	3850	−70	2770
7			−3173	3100	170	3930	−60	2480
8			−3193	3130	180	4000	−70	2520
10			−3098	3300	210	3560	−80	2360
11			−3418	3340	190	3630	−90	3120

[a]Data for $[Pt_3H(\mu_3\text{-}S)(\mu\text{-dppm})_3]^+$.

the dppm ligands. A broad triplet at $\delta = 4.1$ ppm is assigned to the $P_2CH^aH^b$ protons of the two dppm ligands which bridge non-bonded platinum centres, while a multiplet resonance at $\delta = 5.4$ is due to $P_2CH^cH^d$ protons of the third dppm ligand. Since the H^aH^b and H^cH^d protons should be inequivalent in **2**, the complex must be fluxional. Rapid inversion at sulfur, with a planar $Pt_3Me(\mu_3\text{-}S)$ intermediate, leads to apparent equivalence and will be discussed below.

The $^{31}P\{^1H\}$ NMR spectrum of **2** is depicted in Fig. 1 and is assigned by analogy with related clusters (Table 2) [9–11]. In addition to the expected PP and PtP couplings, it is also possible to determine $^1J(PtPt) = 2842$ Hz for the Pt–Pt bond, since the P^c signal is accompanied by ^{195}Pt satellites due to the isotopomer with two ^{195}Pt nuclei. The ^{195}Pt–^{195}Pt couplings observed for other Pt(I) complexes with Pt–Pt bonds are in the range 2400–9100 hz [12].

The $^{195}Pt\{^1H\}$ NMR spectrum of **2** contained two resonances. A doublet of doublets is due to the platinum(I) centers and a triplet is due to the platinum(II) center. Correlation of $^1J(PtP)$ values obtained from the ^{31}P and ^{195}Pt NMR spectra confirms the assignments. It is clear from the data given in Tables 1 and 2 that the clusters **2–5** have very similar structures.

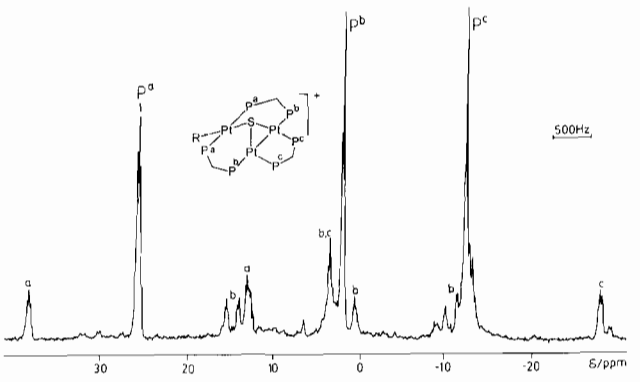

Fig. 1. The ^{31}P NMR spectrum of cation **2**.

Synthesis and characterization of Pt_2M clusters with $M = Pd(II)$, $Rh(I)$ or $Ir(I)$

Heteronuclear clusters with similar structures to **2–5** were prepared by reaction of **1** with other d^8 metal complexes. Thus one of the first known Pt_2Pd clusters $[Pt_2PdCl(\mu_3\text{-}S)(\mu\text{-dppm})_3][Cl]$ (**6a**) was prepared by reaction of **1** with $[PdCl_2(PhCN)_2]$ and isolated as a stable orange solid (Scheme 1) [4, 8, 13]. The chloride salt **6a** could be converted by a simple anion exchange reaction, using NH_4PF_6 in methanol, to the hexafluorophosphate salt **6b**.

Similarly, reaction of **1** with $[Rh(\mu\text{-}Cl)(CO)_2]_2$ or $[Ir(\mu\text{-}Cl)(CO)_3]_2$ gave the Pt_2Rh and Pt_2Ir clusters $[Pt_2M(CO)(\mu_3\text{-}S)(\mu\text{-dppm})_3][Cl]$ (M = Rh (**7a**), Ir (**8**)) (Scheme 1). The reaction forming **7a** was complete within 30 min but the reaction forming **8** required 4 h for completion. Cluster **8** was air-sensitive but was stable when kept under an inert atmosphere.

The products **6–8** were readily characterized by their NMR spectra (Tables 1 and 2). For example, the $^{31}P\{^1H\}$ NMR spectra of **6a** and **6b** were essentially identical. Each contained three resonances, of which two displayed $^1J(PtP)$ couplings and one did not. The PdP resonance was therefore assigned easily; the absence of long-range ^{195}Pt satellites for this signal suggests the lack of any interaction between the palladium and the two platinum centers.

The $^{31}P\{^1H\}$ NMR spectrum of **7a** is shown in Fig. 2. The two upfield signals at $\delta = -9.3$ and 4.22, each with $^1J(PtP)$ couplings, were assigned to the PtP^c and PtP^b phosphorus nuclei, respectively. These resonances have similar patterns to those of **2** (Fig. 1). The signal at $\delta = 27.0$ appears as a multiplet due to coupling to PP couplings but an additional doublet splitting is clearly due to $^1J(^{103}RhP)$. The $^{195}Pt\{^1H\}$ NMR spectrum of **7** is depicted in Fig. 3. As expected there was a single

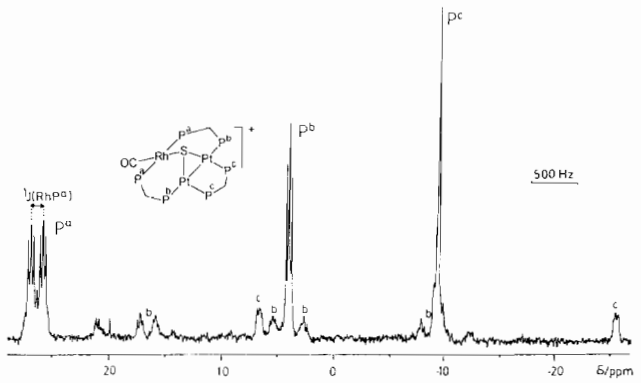

Fig. 2. The ^{31}P NMR spectrum of complex **7**.

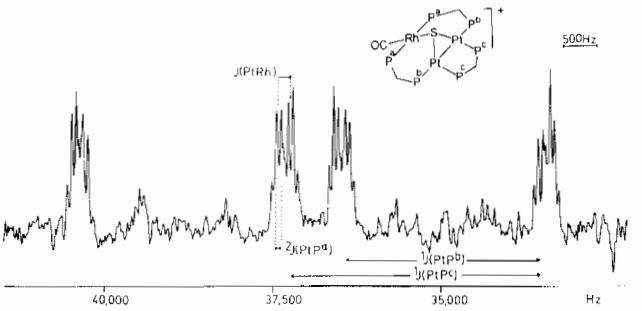

Fig. 3. The ^{195}Pt NMR spectrum of **7**. The RhPt coupling constant is shown.

resonance, and all couplings $^1J(PtP)$, $^2J(PtP)$ were resolved. In addition, a doublet splitting due to the coupling $J(RhPt)$ was readily identified. The presence of the carbonyl ligand in **7a** was confirmed by the IR spectrum, which contained a peak due to the terminal carbonyl with $\nu(CO) = 1973\ cm^{-1}$. In order to establish the ionic nature of **7a**, the hexafluorophosphate salt **7b** was prepared. Its NMR spectra were identical to those of **7a**. Complex **8** was characterized in a similar way. All the d^8 complexes were fluxional, undergoing rapid inversion at the sulfide ligand (Table 1).

Synthesis of Pt_2M clusters with M = Cu(I), Ag(I), Au(I) or Hg(II)

Complex **1** reacted easily with the d^{10} metal compounds CuCl, $AgNO_3$, $[AuCl(SMe_2)]$ and $Hg(NO_3)_2$ to yield trinuclear complexes **9–12** according to Scheme 2. The products were characterized by NMR, MS and elemental analysis. Since the NMR spectra for these clusters are similar, as an example, only the spectra of the Pt_2Au cluster **11** will be discussed in detail. The $^{31}P\{^1H\}$ NMR data for the other clusters are recorded in Table 2. The ^1H NMR spectrum of **11** contained four complex resonances at $\delta = 3.7$, 5.4, 5.8 and 6.5 with an intensity ratio of 2:1:2:1 due to the four types of chemically inequivalent P_2CH_2 protons. A decoupling experiment showed that the signals at $\delta = 3.7$ and 5.8 and those at $\delta = 5.4$ and 6.5 ppm were coupled to each other. Hence, the former two resonances must be due to the H^a and H^b nuclei, while the latter two signals are assigned to the H^c and H^d protons. The presence of four signals for the methylene protons indicates that **11** does not undergo inversion at the sulfide.

The $^{31}P\{^1H\}$ NMR spectrum of **11** is shown in Fig. 4. The assignment of the three resonances was straightforward. The singlet at $\delta = -13.2$, with $^1J(PtP)$ and $^2J(PtP)$ values of 3634 and -80 Hz, respectively, is due to the P^c nuclei of the dppm ligand which bridges the two platinum centres and the negative value for $^2J(PtP^c)$ suggests that the platinum centres are bonded

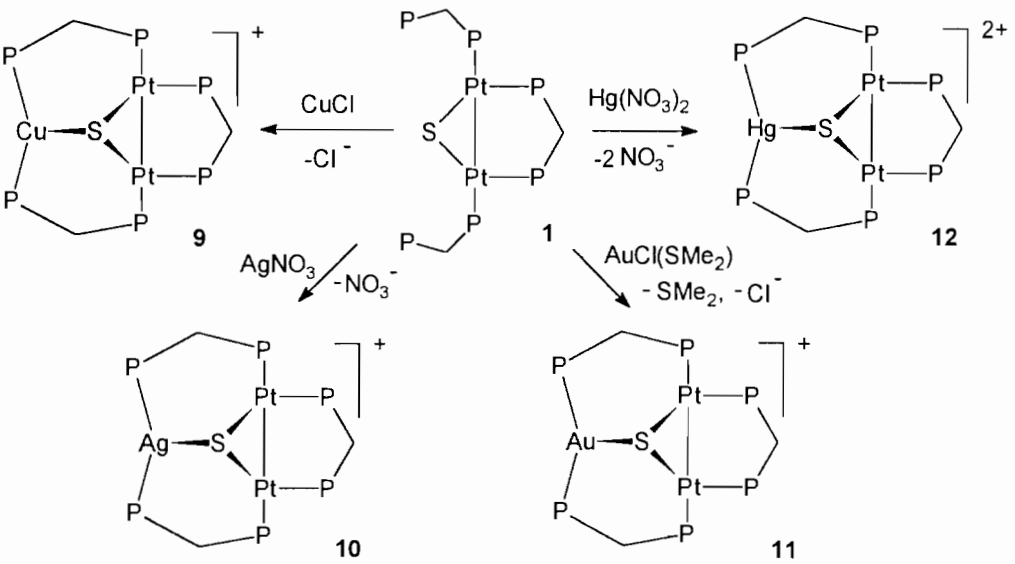

Scheme 2.

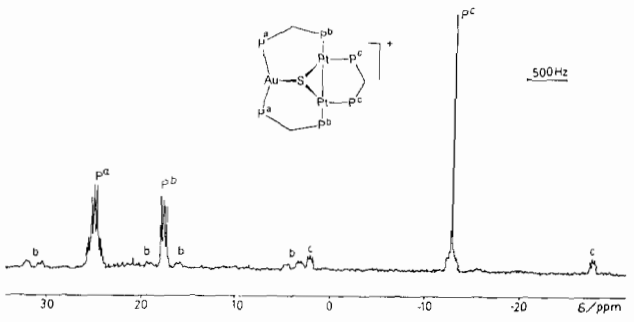

Fig. 4. The ^{31}P NMR spectrum of complex **11**.

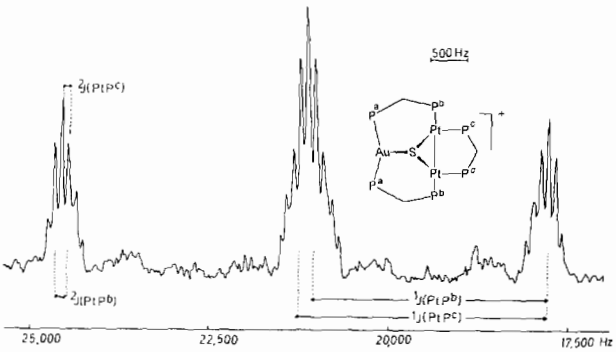

Fig. 5. The ^{195}Pt NMR spectrum of complex **11**.

to each other. Analysis of this signal gives a value for $^1J(PtPt) = 3146$ Hz, thus confirming the presence of a Pt–Pt bond. The two multiplet signals at $\delta = 17.2$ and 24.5 are assigned to P^b and P^a nuclei, respectively. The assignment is clear since only the P^b resonance has satellites due to $^1J(PtP)$ coupling.

The $^{195}Pt\{^1H\}$ NMR spectrum of **11** is shown in Fig. 5. This spectrum appears as a triplet, since $^1J(PtP^b)$ and $^1J(PtP^c)$ are approximately equal, of multiplet resonance at $\delta = -3418$ ppm. Analysis of this resonance gives values of $^1J(Pt–P)$ and $^2J(PtP)$, which agree with the values obtained from the $^{31}P\{^1H\}$ NMR spectrum.

The NMR data described above show that the structure of complex **11** contains a Pt_2Au triangle whose edges are bridged by dppm ligands and that the two platinum atoms are bonded to each other. However, since gold(I) usually prefers linear geometry with coordination number two, there is some question about whether the sulfide ligand is coordinated to gold [14, 15]. In order to answer this question, an X-ray structure determination was carried out. The crystal decomposed in the X-ray beam and the structure was disordered. As a result of these problems, the structure is not precise but the geometry of the cation, which is the issue of chemical interest, is clear.

The inner coordination sphere of the cation $[Pt_2Au(\mu_3\text{-}S)(\mu\text{-dppm})_3]^+$, is illustrated in Fig. 6, and selected bond distances and bond angles are recorded in Table 4. The three metal atoms in **11** define a

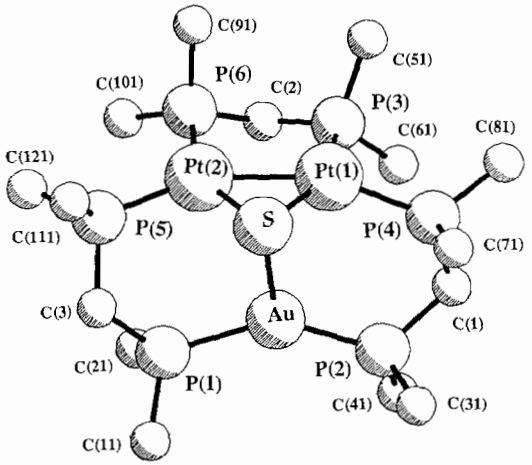

Fig. 6. A view of the structure of complex cation **11**.

TABLE 4. Selected bond distances and angles for $[Pt_2Au(\mu_3\text{-}S)(\mu\text{-dppm})_3]^+$

Bond distances			
Au–Pt1	3.259(2)	Pt1–P4	2.250(10)
Au–Pt2	3.113(2)	Pt2–S	2.301(8)
Au–S	2.621(8)	Pt2–P5	2.275(9)
Au–P1	2.326(9)	Pt2–P6	2.245(9)
Au–P2	2.354(10)	P1–P5	3.10(1)
Pt1–Pt2	2.615(2)	P2–P4	3.19(1)
Pt1–S	2.292(8)	P3–P6	3.03(1)
Pt1–P3	2.253(9)		
Bond angles			
Pt1–Au–Pt2	48.41(4)	Au–Pt2–Pt1	68.72
Pt1–Au–S	44.2(2)	Au–Pt2–S	55.5(2)
Pt1–Au–P1	133.0(2)	Au–Pt2–P5	91.1(2)
Pt1–Au–P2	79.0(2)	Au–Pt2–P6	115.2(2)
Pt2–Au–S	46.4(2)	Pt1–Pt2–S	55.1(2)
Pt2–Au–P1	85.6(2)	Pt1–Pt2–P5	156.9(2)
Pt2–Au–P2	127.2(2)	Pt1–Pt2–P6	95.7(3)
S–Au–P1	113.3(3)	S–Pt2–P5	104.6(3)
S–Au–P2	101.7(3)	S–Pt2–P6	150.7(3)
P1–Au–P2	143.9(3)	P5–Pt2–P6	103.2(3)
Au–Pt1–Pt2	62.87(5)	Au–S–Pt1	82.9(3)
Au–Pt1–S	53.0(2)	Au–S–Pt2	78.1(2)
Au–Pt1–P3	121.2(2)	Pt1–S–Pt2	69.4(2)
Au–Pt1–P4	96.7(3)	Au–P1–P5	90.5(3)
Pt2–Pt1–S	55.5(2)	Au–P2–P4	96.5(4)
Pt2–Pt1–P3	94.3(3)	Pt1–P3–P6	85.1(3)
Pt2–Pt1–P4	154.5(2)	Pt1–P4–P2	82.1(3)
S–Pt1–P3	149.4(3)	Pt2–P5–P1	86.7(3)
S–Pt1–P4	100.7(3)	Pt2–P6–P3	84.1(3)
P3–Pt1–P4	110.0(3)		

triangle. The Pt(1)–Pt(2) distance of 2.615(2) Å is in the range expected for a single bond [3]. While the Pt(1)–Au distance of 3.259(2) Å is definitely out of the range normally associated with platinum–gold bonds, the Pt(2)–Au distance of 3.113(2) Å is just on the limit of those distances which have been associated with weak metal–metal bonding in clusters, and those molecules where weak gold–gold interactions have been

invoked [14–16]. For example, the average gold–gold bond distance in $[(AuPPh_3)_3S][PF_6]$, which is believed to have weak gold–gold bonding, is 3.175(3) Å [16]. For **11**, it is likely that the short Pt–Au distance arises as a consequence of the presence of μ-dppm bridges and not due to metal–metal bonding.

The average Pt–S bond distance in **11** has a normal value of 2.296(8) Å but the Au–S distance of 2.621(8) Å is longer than distances normally associated with Au–S bonds in linear gold complexes. For example, in complexes where the only bonds to gold are from sulfur, the bond lengths are in the range 2.28–2.30 Å [15–17]. In linear complexes when the gold is bonded to a μ_3-S ligand, the bond lengths are longer and vary from 2.30 to 2.34 Å [14–16]. There are no examples of linear gold complexes in which the Au–S bonds exceed 2.41 Å [14–16]. Although the Au–S distance of 2.621(8) Å is long, the P(1)–Au–P(2) angle of 143.9(3)° clearly shows a deviation from linearity. With S–Au–P(1) and S–Au–P(2) angles of 113.3(3) and 101.7(3)°, the gold center has distorted trigonal planar geometry and gold–sulfur bonding is clearly indicated.

Gold(1) and mercury(II) have less tendency to increase their coordination number beyond two than do copper(I) and silver(I) [17]. Since the gold center in **11** is trigonal planar and since the NMR data for the Cu, Ag and Hg analogs **9**, **10** and **12** are similar to those of **11**, it is reasonable to assume that the d^{10} metal centres in all these complexes are also three-coordinate.

μ_3-S inversion in Pt_3 and Pt_2M complexes

The ^1H NMR spectra of the Pt_2M complexes **2–8**, in which M is a d^8 metal ion, contain only two resonances in 2:1 intensity ratio for the P_2CH_2 protons of the dppm ligands. Due to the presence of a μ_3-S bridge, it is not possible for the $Pt_2M(\mu\text{-dppm})_3$ units to have a plane of symmetry containing the PCP atoms of a dppm ligand and, therefore, each of the methylene proton resonances would be expected to appear as an AB quartet due to the non-equivalence of the $P_2CH^aH^b$ and $P_2CH^cH^d$ protons. A variable temperature ^1H NMR study has been carried out for all these clusters. In all cases, as the temperature is lowered, the P_2CH_2 signals broaden and finally split into the expected AB quartets. Clearly, these complexes are fluxional and undergo rapid inversion of the $Pt_2M(\mu_3\text{-S})$ unit to generate an effective plane of symmetry containing the $Pt_2M(\mu_3\text{-S})(\mu\text{-PCP})_3$ atoms at room temperature (eqn. (1)) as previously shown for $[Pt_3H(\mu_3\text{-S})(\mu\text{-dppm})_3]^+$ and related complexes [9–11].

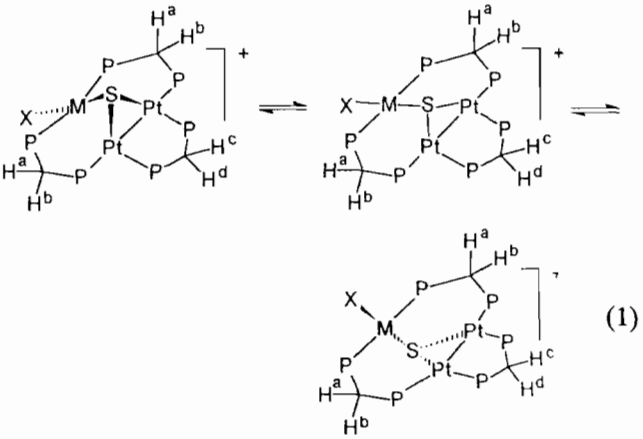

(1)

The activation energies, $\Delta G^{\neq}$, for inversion were calculated by applying the Eyring equation and are listed in Table 1. These are comparable to values reported in the literature for similar complexes. It appears that the $\Delta G^{\neq}$ values for the homonuclear clusters, **2–5**, and the mixed platinum–palladium complex, **6**, are almost independent of the *trans*-influence of the R group or the substitution of platinum for palladium, in contrast to sulfur inversions in dialkyl sulfide or alkanethiolate complexes [18]. It is possible that weakening of the M–S bond *trans* to R should reduce the activation energy to inversion [18], but that the longer M–S bond causes more strain in the bridging dppm ligands in the transition state and that these two effects cancel out. However, significantly lower $\Delta G^{\neq}$ values are observed for **7** and **8** which contain the good π-acceptor carbonyl ligand on rhodium or iridium (Table 1). This observation may be understood in terms of stabilization of the transition state in sulfur inversion by overlap of the empty π^* orbitals of the CO ligand with the filled d_π and p_π orbitals of the metal and the sulfide ligand as shown in **13** (eqn. (2)). Such stabilization of trigonal planar sulfur by π-donation to carbonyl is not possible for the Pt_3 and Pt_2Pd clusters **2–5** and hence higher activation energies for sulfur inversion are observed.

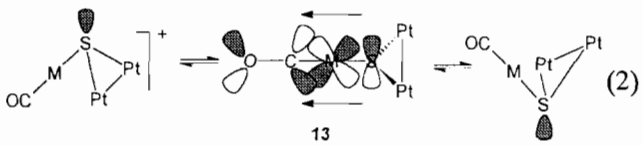

13

(2)

The complexes **9–12** are not fluxional implying that there is a significantly higher activation to inversion. This difference can be attributed to the trigonal planar geometry of the d^{10} metal atom. For the μ_3-S inversion to occur, there has to be a planar transition state and this would require either a distortion of the geometry to T-shaped with *trans* phosphorus donors (structure **14**) or to a significant increase in angle strain of the

μ-dppm ligands (structure **15**) or a combination of both effects (eqn. (3)). The most common distance between the two phosphorus atoms of a μ-dppm ligand is ~3 Å and the P...P distances for the μ-dppm ligands in **11** are 3.09 and 3.19 Å. The $\Delta G^{\ddagger}$ for sulfur inversion via either structure **14** or **15** is therefore expected to be high. It is also noted that the chemical shifts for the P_2CH_2 protons in **9–12** are considerably different from those for **2–8**, perhaps due to the difference in geometry of the d^8 and d^{10} metal centres which affects the conformation of the bridging dppm ligands.

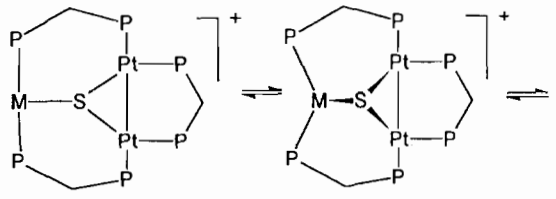

14

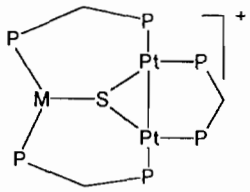

15 (3)

Reactions of Pt_3 and Pt_2M clusters

The μ_3-S ligand in the complexes **2–12** still has one lone pair of electrons and so could act as a nucleophile or as a donor to another metal atom. The Pt_2Rh and Pt_2Ir complexes **7a** and **8** each reacted with excess iodomethane to yield stable complexes characterized as $[Pt_2M(\mu_3\text{-SMe})(CO)(\mu\text{-dppm})_3]I_2$ (**16** and **17**) (Scheme 3). These complexes were readily characterized by their spectroscopic properties.

For example, the ^1H NMR spectrum of **17** contained a triplet signal due to the SMe protons at $\delta = 1.78$, with broad ^{195}Pt satellites. The P_2CH_2 protons appeared as two sets of AB quartets in the region $\delta = 4.3$–5.8, showing that inversion at sulfur is no longer possible. The $^{31}P\{^1H\}$ NMR spectrum contained the expected three resonances and data are given in 'Experimental'. The IR spectrum confirmed the presence of the terminal carbonyl, $\nu(CO) = 2047$ cm^{-1}, and the mass spectrum gave a peak envelope at $m/z = 1937$, which corresponds to the molecular weight of the cation. The loss of the carbonyl and methyl groups is indicated by peaks at 1909 and 1893, respectively. Finally, the elemental analysis indicates that the counterions are I^-.

The complexes **5**, **7a** and **8** were treated with $AgBF_4$ with the intention of forming AgCl and the BF_4^- salts of the complexes. However, very little AgCl was precipitated and the analytical data showed that AgCl was incorporated into the products. It was originally believed [8] that the AgCl was complexed by the μ^3-S ligand as in **18** but, following the characterization of a similar complex cation $[Pt_3(\mu_3\text{-S})(AuPPh_3(\mu_3\text{-AgCl})(\mu\text{-dppm})_3]^+$ [19], the products are now believed to be **19** and **20** (Scheme 3). Data for **20** will be discussed.

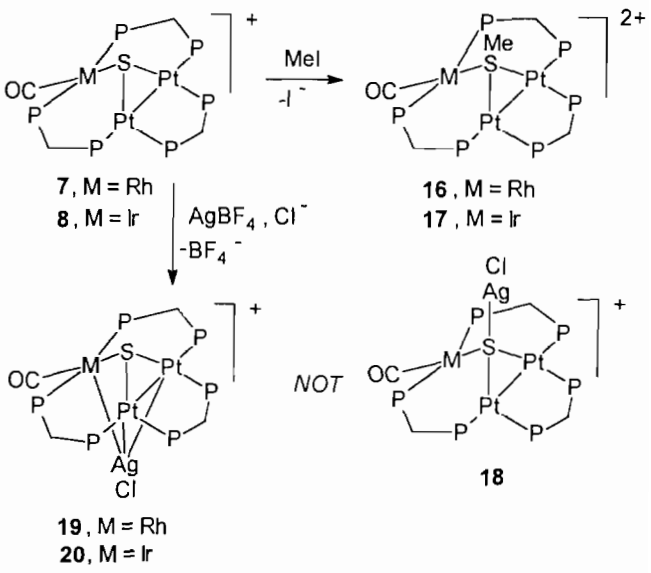

Scheme 3.

The $^{31}P\{^1H\}$ NMR spectrum of **20** contained the expected three signals ('Experimental') and the ^1H NMR spectrum contained two sets of AB quartets, indicating that inversion at sulfur does not occur. These data can be interpreted in terms of either structure **18** or **20**. The $^{195}Pt\{^1H\}$ NMR spectrum of **20** contained a single resonance, which displayed the expected couplings to ^{31}P and ^{103}Rh and an extra doublet splitting assigned as $^1J(AgPt) = 400$ Hz. The resonance was too broad to give resolved ^{195}Pt–^{107}Ag and ^{195}Pt–^{109}Ag couplings, but the coupling lies in the range of known $^1J(PtAg)$ couplings of 190–680 Hz [20–22]. This leads to the conclusion that structure **20** is correct, since **18** would surely give a lower coupling $^2J(PtAg)$.

It is interesting that methyl iodide reacts with the nucleophilic sulfide but that AgCl adds to the Pt_2M atoms. There are now many examples of stable complexes in which electrophilic silver(I) adds to electron-rich platinum complexes [23].

Experimental

The complex $[Pt_2(\mu\text{-S})(\mu\text{-dppm})(\eta^1\text{-dppm})_2]$ was prepared as described previously [7].

[$Pt_3Me(\mu_3\text{-}S)(\mu\text{-}dppm)_3$][Cl]

To a solution of [$Pt_2(\mu\text{-}S)(\mu\text{-}dppm)(\eta^1\text{-}dppm)_2$] (0.06 mmol) in acetone (5 ml) was added *trans*-[$PtClMe(SMe_2)_2$] (0.06 mmol) in acetone (5 ml). The reaction mixture was stirred for 30 min after which time the volume of the solution was reduced. Pentane (10 ml) was added and the product was precipitated as a yellow solid. This was separated, washed several times with pentane (10 ml) and dried *in vacuo*. Yield 95%; m.p. 206 °C dec. *Anal.* Calc. for $C_{76}H_{69}ClP_6Pt_3S$: C, 47.3; H, 4.2. Found: C, 47.3; H, 4.0%. MS: $m/z = 1785$ ($P-Cl$), 1770 ($P-Cl$, Ph).

The following were prepared similarly.

[$Pt_3Ph(\mu_3\text{-}S)(\mu\text{-}dppm)_3$][Cl] from *trans*-[$PtClPh(SMe_2)_2$]: yield 90%; m.p. 205 °C dec. *Anal.* Calc. for $C_{81}H_{71}ClP_6Pt_3S$: C, 51.6; H, 3.8. Found: C, 50.9; H, 4.0%. MS: $m/z = 1848$ ($P-Cl$), 1771 ($P-Cl$, Ph).

[$Pt_3(CH_2Cl)(\mu_3\text{-}S)(\mu\text{-}dppm)_3$][Cl] from [$PtCl(CH_2Cl)(cod)$]; yield 90%; m.p. 220 °C dec. *Anal.* Calc. for $C_{76}H_{68}Cl_2P_6Pt_3S$: C, 49.2; H, 3.7. Found: 48.9; H, 4.1%. MS: $m/z = 1820$ ($P-Cl$).

[$Pt_3Cl(\mu_3\text{-}S)(\mu\text{-}dppm)_3$][Cl] from [$PtCl_2(SMe_2)_2$]; yield 80%; m.p. 210 °C dec. *Anal.* Calc. for $C_{75}H_{66}Cl_2P_6Pt_3S$: C, 48.9; H, 3.6. Found: C, 48.7; H, 3.7%. MS: $m/z = 1806$ ($P-Cl$).

[$Pt_2PdCl(\mu_3\text{-}S)(\mu\text{-}dppm)_3$][Cl]

To a solution of [$Pt_2(\mu\text{-}S)(\mu\text{-}dppm)(\eta^1\text{-}dppm)_2$] (45 mg, 0.03 mmol) in acetone (5 ml) was added [$PdCl_2(NCPh)_2$] (11 mg, 0.03 mmol). An immediate reaction led to a color change from yellow to orange. The mixture was stirred for 30 min. After reducing the volume and addition of pentane (10 ml), orange microcrystals of the product were obtained. These were further washed with pentane (10 ml) and dried *in vacuo* Yield 96%; m.p. 220 °C dec. *Anal.* Calc. for $C_{75}H_{66}Cl_2P_6PdPt_2S$: C, 51.4; H, 3.8. Found: C, 50.8; H, 3.7%. MS: *m/z*1717 ($P-Cl$), 1682 ($P-2Cl$).

[$Pt_2Rh(CO)(\mu_3\text{-}S)(\mu\text{-}dppm)_3$][Cl]

This was prepared in a similar way from [$Rh(CO)_2(\mu\text{-}Cl)]_2$ (7 mg, 0.02 mmol) in acetone (3 ml), and isolated as an orange microcrystalline product. Yield 85%; m.p. 240 °C dec. *Anal.* Calc. for $C_{76}H_{66}ClOP_6Pt_2RhS$: C, 52.4; H, 3.8. Found: C, 51.5; H, 4.0%. MS: $m/z = 1742$ (P), 1706 ($P-Cl$) 1678 ($P-Cl$, CO). IR: $\nu(CO) = 1973$ cm^{-1}.

[$Pt_2Ir(CO)(\mu_3\text{-}S)(\mu\text{-}dppm)_3$][Cl]

This was prepared in a similar way from a suspension of [$Ir(CO)_3(\mu\text{-}Cl)]_2$ (10 mg, 0.01 mmol) in acetone (3 ml) for 3 h, and isolated as a yellow solid. Yield 90%; m.p. 265 °C dec. *Anal.* Calc. for $C_{76}H_{66}ClOP_6IrPt_2S$: C, 49.8; H, 3.6. Found: C, 48.9; H, 3.8%. MS: $m/z = 1831$ (P), 1796 ($P-Cl$), 1766 ($P-Cl$, CO). IR: $\nu(CO) = 1970$ cm^{-1}.

[$Pt_2Cu(\mu_3\text{-}S)(\mu\text{-}dppm)_3$][Cl]

A suspension of CuCl (2 mg, 0.02 mmol) in CH_2Cl_2 (3 ml) was added to a solution of [$Pt_2(\mu\text{-}S)(\mu\text{-}dppm)(\eta^1\text{-}dppm)_2$] (36 mg, 0.02 mmol) in acetone (5 ml). The mixture was stirred for 1 h giving a homogeneous solution. The volume of the solution was reduced and addition of pentane (10 ml) gave the product as a yellow microcrystalline solid. Yield 80%; m.p. 234 °C dec. *Anal.* Calc. for $C_{75}H_{66}ClCuP_6Pt_2S$: C, 53.8; H, 3.9. Found: C, 53.6; H, 3.9%. MS: $m/z = 1638$ ($P-Cl$). ^1H NMR (in d_6-benzene): δ (ppm) = 2.26 [m, 2H, $P_2CH^aH^b$], 3.34 [m, 1H, $P_2CH^cH^d$], 4.01 [m, 2H, $P_2CH^aH^b$], 4.6 [m, 1H, $P_2CH^cH^d$], 6.9–7.3 [m, 60H, Ph].

[$Pt_2Ag(\mu_3\text{-}S)(\mu\text{-}dppm)_3$][$NO_3$]

This was prepared in a similar way from Ag NO_3 and isolated as a yellow microcrystalline solid. Yield 80%; m.p. 240 °C dec. *Anal.* Calc. for $C_{75}H_{66}AgNO_3P_6Pt_2S$: C, 51.6; H, 3.8. Found: C, 50.8; H, 4.0%. MS: $m/z = 1683$ ($P-NO_3$). ^1H NMR (in $CDCl_3$): δ (ppm) = 2.34 [m, 2H, $P_2CH^aH^b$], 3.75 [m, 2H, $P_2CH^aH^b$], 4.25 [m, 1H, $^2J(PH) = 12$ Hz, $P_2CH^cH^d$], 5.94 [m, 1H, $P_2CH^cH^d$], 6.9–7.3 [m, 60H, Ph].

[$Pt_2Au(\mu_3\text{-}S)(\mu\text{-}dppm)_3$][Cl]

This was prepared similarly from [$AuCl(SMe_2)$]. Yield 80%; m.p. 240 °C dec. *Anal.* Calc. for $C_{75}H_{66}AuClP_6Pt_2S$: C, 49.8; H, 3.7. Found: C, 49.1; H, 3.7%. MS: $m/z = 1772$ ($P-Cl$). ^1H NMR (in d_6-acetone): δ (ppm) = 2.45 [m, 2H, $P_2CH^aH^b$], 4.38 [m, 1H, $^2J(HH) = 12$ Hz, $P_2CH^cH^d$], 4.82 [m, 2H, $^2J(HH) = 12$ Hz, $P_2CH^aH^b$], 6.12 [m, 1H, $P_2CH^cH^d$], 6.9–7.3 [m, 60H, Ph].

[$Pt_2Hg(\mu_3\text{-}S)(\mu\text{-}dppm)_3$][$NO_3$]$_2$

This was prepared similarly from $Hg(NO_3)_2 \cdot H_2O$. Yield 81%; m.p. 275 °C dec. *Anal.* Calc. for $C_{75}H_{66}N_2HgO_6P_6Pt_2S$: C, 47.4; H, 3.5; N, 1.4. Found: C, 47.5; H, 3.6; N, 1.3%. MS: $m/z = 1776$ ($P-2NO_3$). ^1H NMR: $\delta = 2.95, 3.99, 4.21, 5.89$ [each m, 2H, CH_2P_2].

[$Pt_2PdCl(\mu_3\text{-}S)(\mu\text{-}dppm)_3$][$PF_6$]

A solution of the chloride salt in acetone was added dropwise to a saturated solution of NH_4PF_6 in methanol (5 ml). The product precipitated and was isolated by filtration and washed with water (10 ml) to remove excess NH_4PF_6. The remaining orange solid was washed with pentane (10 ml) and dried under vacuum. *Anal.* Calc. for $C_{75}H_{66}ClF_6P_7PdPt_2S$: C, 48.4; H, 3.6. Found: C, 47.9; H, 3.7%.

[$Pt_2Rh(CO)(\mu_3$-S)(μ-dppm)$_3$][PF_6]

This was prepared by a similar procedure. Yield 70%; m.p. 260 °C dec. *Anal.* Calc. for $C_{76}H_{66}F_6OP_7SPt_2Rh$: C, 49.3; H, 3.6. Found: C, 48.6; H, 3.8%.

[$Pt_2Rh(CO)(\mu_3$-SMe)(μ-dppm)$_3$][I]$_2$

To a solution of [$Pt_2Rh(CO)(\mu_3$-S)(μ-dppm)$_3$][Cl] (50 mg, 0.03 mmol) in acetone (5 ml) was added MeI (40 mg, 0.3 mmol). The mixture was stirred for 2 h. Solvent was removed *in vacuo*. The oily residue was dissolved in acetone (3 ml) and the product was precipitated by addition of pentane (10 ml). The product was collected, washed with pentane (15 ml) and dried. Yield 66%; m.p. 270 °C. *Anal.* Calc. for $C_{77}H_{69}I_2OP_6Pt_2RhS$: C, 46.8; H, 3.5. Found: C, 45.9; H, 3.8%. MS: *m/z* = 1960 (*P* − Me), 1932 (*P* − Me, CO), 1804 (*P* − Me, CO, I). IR: ν(CO) = 1948 cm^{-1}. ^{1}H NMR (in d_6-acetone): δ (ppm) = 1.92 [m, 3H, ^4J(PH) = 6, MeS], 3.60 [m, 2H, $P_2CH^aH^b$], 3.81 [m, 2H, $P_2CH^aH^b$], 4.88 [m, 1H, $P_2CH^cH^d$], 4.92 [m, 1H, $P_2CH^cH^d$], 6.90 − 7.27 [m, 60H, Ph]. $^{31}P\{^1H\}$ NMR (in d_6-acetone): δ (ppm) = −8.8 [br s, 2P, ^1J(PtP) = 3850 Hz, P^c], −3.2 [t, 2P, J(PP) = 17, $^3J(P^bP^{b'})$ = 175, ^1J(PtP) = 3100, ^2J(PtP) = 150 Hz, P^b], 20.9 [d of m, 2P, ^1J(RhP) = 116 Hz, P^a].

[$Pt_2Ir(CO)(\mu_3$-SMe)(μ-dppm)$_3$][I]$_2$

This was prepared in a similar way. Yield 65%; m.p. 280 °C dec. *Anal.* Calc. for $C_{77}H_{69}I_2IrOP_6Pt_2S$: C, 44.8; H, 3.4. found: C, 44.3; H, 3.4%. MS: *m/z* = 1937 (*P* − I), 1909 (*P* − I, CO), 1894 (*P* − I, CO, Me). IR: ν(CO) = 2046 cm^{-1}. ^{1}H NMR (in d_6-acetone): δ (ppm) = 1.78 [t, 3H, ^3J(PtH) = 48, ^4J(PH) = 6 Hz, MeS], 3.61 [m, 2H, $P_2CH^aH^b$], 3.92 [m, 2H, $P_2CH^aH^b$], 4.32 [m, 1H, $P_2CH^cH^d$], 5.8 [m, 1H, $P_2CH^cH^d$], 6.9–7.3 [m, 60 H, Ph]. $^{31}P\{^1H\}$ NMR (in d_6-acetone): δ (ppm) = −18.1 [m, 2P, P^a], −10.4 [m, 2P, ^1J(PtP) = 3925 Hz, P^c], −1.9 [m, 2P, ^1J(PtP) = 3150, ^1J(PtP) = 125, ^3J(PP) = 175 Hz, P^b].

[$Pt_3Cl(\mu_3$-S)(μ_3-AgCl)(μ-dppm)$_3$][BF_4]

To a solution of [$Pt_3Cl(\mu_3$-S)(μ-dppm)$_3$][Cl] (40 mg, 0.02 mmol) in acetone (5 ml) was added $AgBF_4$ (4 mg, 0.02 mmol) in the absence of light. An immediate reaction was evident from the color change. The mixture was stirred for 30 min. The volume of the solution was reduced and addition of pentane (10 ml) resulted in the precipitation of the product as a yellow microcrystalline solid. The product was washed with pentane (10 ml) and dried *in vacuo*. Yield 50%; m.p. 260 °C dec. *Anal.* Calc. for $C_{75}H_{66}AgBCl_2F_4P_6Pt_3S$: C, 44.2; H, 3.3. Found: C, 44.0; H, 3.1%. ^{1}H NMR (in d_6-acetone): δ (ppm) = 4.04 [m, 2H, $P_2CH^aH^b$], 4.12 [m, 2H, $P_2CH^aH^b$], 5.76 [m, 1H, $P_2CH^cH^d$], 5.90 [m, 1H, $P_2CH^cH^d$], 6.9–73. [m, 60H, Ph]. $^{31}P\{^1H\}$ NMR (in d_6-acetone): δ (ppm) = −11.1 [s, 2P, ^1J(PtP) = 3700 Hz, P^c], 11.0 [t, 2P, ^2J(PP) = 20, ^3J(PP) = 170, ^1J(PtP) = 3150, ^2J(PtP) = 170 Hz, P^b], 25.9 [t, ^1J(PtP) = 2600 Hz, P^a].

[$Pt_2Rh(CO)(\mu_3$-S)(μ_3-AgCl)(μ-dppm)$_3$][BF_4]

This was prepared in a similar way. Yield 65%; m.p. 270 °C dec. *Anal.* Calc. for $C_{76}H_{66}AgBClF_4OP_6Pt_2RhS$: C, 47.1; H, 3.4. Found: C, 46.5; H, 3.1%. MS: *m/z* = 1849 (*P* − BF_4). IR: ν(CO) = 1970 cm^{-1}. ^{1}H NMR (in d_6-acetone): δ(ppm) = 3.92 [m, 2H, $P_2CH^aH^b$], 4.42 [m, 2H, $P_2CH^aH^b$], 5.02 [m, 1H, $P_2CH^cH^d$], 5.98 [m, 1H, $P_2CH^cH^d$], 6.9–7.3 [m, 60H, Ph]. $^{31}P\{^1H\}$ NMR (in d_6-acetone): δ (ppm) = −9.3 [t, 2H, ^2J(PP) = 7, ^1J(PtP) = 3700, ^2J(PtP) = −80 Hz, P^c], 11.1 [m, 2H, ^1J(PtP) = 3100, ^2J(PtP) = 195, ^3J(PP) = 145 Hz, P^b], 31.8 [m, 2H, ^1J(RhP) = 120 Hz, P^a]. $^{195}Pt\{^1H\}$ NMR (in d_6-acetone): δ (ppm) = −2896 [m, ^1J(PtP) = 3700, ^1J(PtP) = 3100, ^1J(PtRh) = 120, ^1J(PtAg) = 380 Hz].

[$Pt_2Ir(CO)(\mu_3$-S)(μ_3-AgCl)(μ-dppm)$_3$][BF_4]

This was prepared in a similar way. Yield 54%; m.p. 260 °C dec. *Anal.* Calc. for $C_{76}H_{66}AgBClF_4IrOP_6Pt_2S$: C, 45.1; H, 3.3. Found: C, 45.2; H, 3.24%. MS: *m/z* = 1903 (*P* − BF_4, Cl). ^{1}H NMR (in d_6-acetone): δ (ppm) = 4.08 [m, 2H, $P_2CH^aH^b$], 4.46 [m, 2H, $P_2CH^aH^b$], 5.46 [m, 2H, $P_2CH^cH^d$], 6.9 − 7.3 [m, 60H, Ph]. $^{31}P\{^1H\}$ NMR (in d_6-acetone): δ (ppm) = −10.1 [s, 2P, ^1J(PtP) = 4000 Hz, P^c], 11.2 [m, 2P, ^1J(PtP) = 3100, ^2J(PtP) = 140, ^3J(PP) = 160 Hz, P^b], 19.1 [m, 2P, P^a].

X-ray analysis of [$Pt_2Au(\mu_3$-S)(μ-dppm)$_3$][Cl]

Transparent yellow crystals were grown by slow evaporation of a solution in acetone. Since the crystals lost solvent when exposed to air, a suitable crystal was coated with epoxy glue. Weissenberg and Precession photography revealed triclinic symmetry. The density was determined by neutral buoyancy in pentane and 1,2-dibromoethane. The density measurement and NMR data indicated that the crystal contained acetone solvent of crystallization.

The single crystal chosen for data collection was coated with epoxy and transferred to an Enraf-Nonius CAD4F diffractometer. The orientation matrix and cell dimensions were determined at $15 \leqslant \theta \leqslant 20$ from 20 high angle reflections. Crystal data and experimental details are found in Table 5 and atom coordinates are listed in Table 6. Intensity data were collected by the θ–2θ scan technique at room temperature and ω scans of several intense reflections were recorded both before and after data collection. Background, and Lorentz and polarization corrections were applied. The data were corrected for absorption to give 6855 unique reflections.

The structure of the cation was solved in space group $P\bar{1}$, No. 2, by Patterson and Fourier methods. The Pt, Au, P, S and Cl atoms were assigned anisotropic thermal

TABLE 5. Summary of X-ray structure determination for $[Pt_2Au(\mu_3\text{-}S)(\mu\text{-}dppm)_3]Cl$

Compound; M_R	$C_{75}H_{66}ClSP_6AuPt_2 \cdot C_3H_6O$; 1866.85
Crystal system; space group	triclinic; $P\bar{1}$
Cell dimensions	
a (Å)	11.913(2)
b (Å)	27.870(6)
c (Å)	11.158(2)
α (°)	92.01(1)
β (°)	95.21(1)
γ (°)	88.87(2)
Cell volume (Å^3); Z	3687(2); 2
D (g cm^{-3}): obs.; calc.	1.76(1); 1.73
Monochromator	graphite
Radiation; wavelength (Å)	Mo, λ(Mo Kα) 0.71073
Crystal dimensions (mm)	0.12×0.16×0.25
No. data; No. standards collected	7334; 152
Corrections	Lorentz and polarization
Decay; absorption correction	yes; Gaussian
Absorption coefficient (mm^{-1})	6.04
No. unique data	6855
R, R_w	0.083, 0.109

TABLE 6. Selected atomic positional and thermal parameters[a]

Atom	x	y	z	U_{eq}[b] or U (Å^2)
Au	3491(1)	2715.1(5)	1395(1)	393(5)
Pt1	4823(1)	1753.0(5)	509(1)	295(4)
Pt2	5351(1)	2566.9(5)	−375(1)	280(4)
S	3596(7)	2228(3)	−646(7)	31(3)
P1	3806(8)	3531(3)	1248(8)	33(3)
P2	2798(8)	2137(4)	2615(8)	38(3)
P3	6597(8)	1582(3)	1269(8)	37(3)
P4	3627(8)	1219(4)	1132(9)	40(3)
P5	5073(8)	3328(3)	−1025(8)	31(3)
P6	7129(7)	2574(4)	486(8)	36(3)
C1	249(3)	151(1)	191(3)	3.4(9)
C2	740(3)	215(1)	170(3)	3.5(9)
C3	494(3)	375(1)	32(3)	3.5(9)

[a]The positional and thermal parameters for the metals are given by $\times 10^4$ and those for the chlorine, sulfur and phosphorus atoms are given by $\times 10^4$ and $\times 10^3$, respectively. The positional and thermal parameters for the remaining carbon atoms are given by $\times 10^3$ and $\times 10^2$, respectively. [b]$U_{eq} = \frac{1}{3}\Sigma_i\Sigma_j U_{ij} a^*_i a^*_j \mathbf{a}_i \cdot \mathbf{a}_j$.

parameters and the C atoms were left isotropic. Partial refinement by block-diagonal least-squares on F, minimizing the function $\Sigma w(\|F_o| - |F_c\|)^2$, where the weight w is given by $4|F_o|/\sigma^2(F_o)^2$, reduced R_1 and R_2 to 0.083 and 0.109, respectively. At this point the connectivity of the cation was determined and a Fourier difference map contained a peak assigned to a chloride anion at the centre of inversion of the cell. Several other peaks were present in the Fourier map, but a good model could not be obtained. Disorder is assumed to occur between the second chlorine anion (required for neutrality) and the acetone of solvation.

Acknowledgement

We thank NSERC (Canada) for financial support.

References

1 R.J. Puddephatt, *Chem. Soc. Rev.*, (1983) 99.
2 B. Chaudret, B. Delavaux and R. Poilblanc, *Coord. Chem. Rev., 86* (1988) 191.
3 R.J. Puddephatt, Lj. Manojlovic-Muir and K.W. Muir, *Polyhedron, 9* (1990) 2767.
4 D.I. Gilmour, M.A. Luke and D.M.P. Mingos, *J. Chem. Soc., Dalton Trans.*, (1987) 335.
5 D.A. Roberts and G.L. Geoffroy, in E.W. Abel, F.G.A. Stone and G. Wilkinson (eds.), *Comprehensive Organometallic Chemistry, Vol. 6,* Pergamon, Oxford, 1982, p. 763.
6 W. Bos, J.J. Bour, P.P.J. Schlebos, P. Hageman, W.P. Bosman, J.M.M. Smits, J.A.C. van Wietmarschen and P.T. Beurskens, *Inorg. Chim. Acta, 119* (1986) 141.
7 N. Hadj-Bagheri and R.J. Puddephatt, *Inorg. Chem., 28* (1989) 2384.
8 N. Hadj-Bagheri and R.J. Puddephatt, *J. Chem. Soc., Chem. Commun.*, (1987) 1269.
9 M.C. Jennings, N.C. Payne and R.J. Puddephatt, *Inorg. Chem., 26* (1987) 3776.
10 A.M. Bradford, M.C. Jennings and R.J. Puddephatt, *Organometallics, 8* (1989) 2367.
11 G. Ferguson, B.R. Lloyd, Lj. Manojlovic-Muir, K.W. Muir and R.J. Puddephatt, *Inorg. Chem., 25* (1986) 4190.
12 M.C. Grossel, J.R. Batson, R.P. Moulding and K.R. Seddon, *J. Organomet. Chem., 304* (1986) 391.

13 C.E. Briant, D.I. Gilmour, M.A. Luke and D.M.P. Mingos, *J. Chem. Soc., Dalton Trans.,* (1985) 851.
14 C.E. Briant, T.S.A. Hor, N.D. Howells and D.M.P. Mingos, *J. Organomet. Chem., 256* (1983) C15.
15 R.J. Puddephatt, in G. Wilkinson (ed.), *Comprehensive Coordination Chemistry,* Vol. 5, Pergamon, Oxford, 198, Ch. 55.
16 P.G. Jones, *Gold Bull., 14* (1981) 102; *19* (1986) 46.
17 R.J. Puddephatt, *The Chemistry of Gold,* Elsevier, Amsterdam, 1978.
18 E.W. Abel, S.K. Bhargava and K.G. Orrell, *Prog. Inorg. Chem., 32* (1984) 1.
19 G. Douglas, M.C. Jennings, Lj. Manojlovic-Muir, K.W. Muir and R.J. Puddephatt, *Inorg. Chem., 27* (1988) 4516.
20 A. Albinati, K.H. Dahmen, A. Togni and L.M. Venanzi, *Angew. Chem., Int. Ed. Engl., 24* (1985) 766.
21 S. Bhaduri, K. Sharma, P.G. Jones and C.F. Erdbrugger, *J. Organomet. Chem., 326* (1987) C46.
22 G.J. Arsenault, C.M. Anderson and R.J. Puddephatt, *Organometallics, 7* (1988) 2094.
23 R. Uson, J. Fornies, M. Tomas, J.M. Casas and R. Navarro, *J. Chem. Soc., Dalton Trans.,* (1989) 169.